

Optical studies of porous glass media containing silver particles

Sung-Ik Lee, Tae W. Noh, and J. R. Gaines

Department of Physics, Ohio State University, Columbus, Ohio 43210-1106

Ying-Hsiang Ko and Eric R. Kreidler

Department of Ceramic Engineering, Ohio State University, Columbus, Ohio 43210

(Received 2 March 1987; revised manuscript received 27 July 1987)

We prepared Ag-glass composites by impregnating porous glass with a AgNO_3 solution. The samples were then reduced (in a hydrogen atmosphere) and densified before they were characterized by x-ray diffraction and electron microscopy. The growth of the metal particles inside the glass was studied by a transmission electron microscope. The optical properties of these composites were studied by measuring the reflectance between 10 000 and 40 000 cm^{-1} . To explain the measured reflection spectra, we used two different theoretical approaches, i.e., the Maxwell-Garnett theory (MGT) and a lattice gas model developed by Persson and Liebsch (PLT). This latter model was more successful in accounting for the red shift, the line broadening, and the reduction of the peak in the reflectance spectra than the MGT. However, our measured spectrum still cannot be explained *quantitatively* by the PLT. In particular, there is a "dip" in the reflection spectra whose position depends on the mean size of the Ag particles. This cannot be explained by either theory.

I. INTRODUCTION

The optical properties of small-metallic-particle systems have been of interest since the beginning of the century when Maxwell-Garnett provided the first theoretical framework¹ to explain the resonant absorption (or dielectric anomaly) which characterizes such systems. Recently, the optical properties of colloidal metal particles in different media (mostly glasses^{2,3} or ionic crystals⁴) have been studied because of their potential technological importance as efficient photothermal solar-energy converters⁵ (among other uses). There is also considerable interest in developing new techniques for making such composite materials.

In the past, composites of metal particles in a glass matrix have been prepared by nucleation of small metal particles with ultraviolet irradiation followed by a suitable heat treatment.² The metal particles in such composites are spherical in shape with typical size of 100 Å and usually the metal volume fraction (p) is very low ($p < 10^{-4}$). A different type of Ag-glass composite was prepared by Sarkar *et al.*⁶ using sodium \rightleftharpoons silver ion exchange followed by reduction treatments in a hydrogen atmosphere. The size of the metal particles produced was between 30 and 500 Å and the particles had roughly elliptical shape. The metal particles were located only near the surface (up to about 2 μm from the surface) with $p \approx 0.04$ in this surface region.

Another class of metal-glass composites called "granular metal films" or "cermets"^{7,8} is prepared by coevaporation or cosputtering techniques. One advantage of granular metal films is that they can be produced with a wide range of metal concentrations so that the metal-insulator transition can be studied systematically in these composites. The metal particles are about 100 Å in size,

but complicated topological changes⁸ occur near the metal-insulator transition.

In addition to these experimental advances, several new "effective-medium theories" have been developed recently.^{9,10} These theories include interactions between the particles of the composite and take into account the disorder in the spatial distribution of particles. Such interactions are neglected in the Maxwell-Garnett theory (MGT).¹ These newer theories usually predict both a red shift and broadening of the dipole resonance, effects which have been observed in some metal-insulator composites.¹¹

Quite recently, Kaiser, Logothetis, and Wegner¹² developed a new experimental technique, the "tandem-sputtering" technique. This method produces composite materials having uniformly sized, spherical particles uniformly dispersed throughout the composite. However, optical measurements on these composites (of simple topology) do not show the red shift of the dipole resonance which is a key feature of the recently developed effective-medium theories.^{9,10} Moreover, they concluded that a simple form of inhomogeneity of the metal-particle electronic structure due to surface effects cannot explain their results.

In this paper we report reflection measurements on a new class of silver glass composites. Electron-microscope studies show the simple topology of these composites. The silver particles are spherical and do not form clusters in contrast to observations in other classes of composites.¹³ These simple topology composites provide us with a very novel system to study by optical techniques. Moreover, we can compare our experimental results with the predictions of the MGT and those of recently developed theories, and reexamine the points of conflict between the recent experiments and the recent

effective-medium theories.

The preparation of the samples, their characterization, and the reflection spectra from the samples are presented in Sec. II. In Sec. III we present a brief review of the two effective-medium theories we use to analyze the spectra. Specifically, our measured reflectance spectra are compared with two different theories, i.e., the Maxwell-Garnett theory¹ (MGT) and an effective-medium theory recently developed by Persson and Liebsch⁹ (PLT) in Sec. IV. Although PLT predicts a red shift, a line broadening, and a reduction of the peak (better than MGT) in the reflection spectrum, we find that some of the optical properties of our composites depend on the mean Ag particle diameter in a way that cannot be explained even by the PLT.

Actually, Mie theory, which is based on the interaction of a planar electromagnetic wave with the spherical particles of arbitrary index of refraction embedded in a dielectric media, can explain the Maxwell-Garnett resonance change as a function of radius. Since Mie theory is a complete theory and not an approximation, it can explain the scattering and absorption of the small particles. It can also explain the change of the dip in the Maxwell-Garnett resonance as a function of the radius of particles. However, Mie theory does not incorporate a material surface so we cannot apply it to the reflection measurement due to the sudden change in dielectric constant at the surface of the composite. For this reason, we did not compare the experimental results for the reflection change for different size particles inside the glass composite with this theory.

II. EXPERIMENTAL PROCEDURE

A. Sample preparation

Ag-deficient glass is a commercially available porous glass¹⁴ which is made from a heat-treated borosilicate glass by leaching out one of the two separated phases, the borate-rich phase, leaving a SiO₂-rich skeleton. The composition of Ag-deficient glass nominally consists of 96 wt. % SiO₂ and 3 wt. % B₂O₃. A series of composite samples was prepared by impregnating Ag-deficient glass, Corning 7910, with various AgNO₃ solutions. The Ag-deficient glass "as-received" was cut into pieces 25 mm square by 6 mm thick. The glass acquires a brown color on standing in air, possibly due to adsorption of organic matter. The brown color could be removed by boiling the glass for 6 h in a solution consisting of 200 ml H₂O₂ (38%) and a few grams of KClO₃. The cleaned glass was rinsed three times in boiling, doubly distilled water and then was stored in doubly distilled water.

The cleaned glass was dried just prior to use by purging with N₂ overnight. The dried glass was impregnated by immersion in AgNO₃ solutions of various concentrations, i.e., 5, 10, and 15 mol %, depending upon the silver concentration desired. The solutions with the samples were kept in a sealed black Teflon container overnight. The impregnated glasses were then dried in an oven at 60°C until no more weight loss was noticed. These dried samples were heated at 220°C for 3 h and

then slowly raised to 450°C to decompose the AgNO₃ (decomposition temperature 444°C). Samples to be fired at temperatures higher than 450°C were preheated at 450°C for 3 h to decompose the AgNO₃ and to form Ag nuclei. The growth of Ag particles was studied carefully by firing the preheated samples at 700, 900, and 1050°C for various time periods. All the heat treatments were done in air.

The final volume fraction p of silver was determined by measuring (1) the weight change that occurred in each of the above processes and (2) the specific gravity of each of the AgNO₃ solutions. The specific gravities of the various AgNO₃ solutions were determined by pycnometry. Assuming that (a) the decomposition of AgNO₃ is complete, (b) no silver is lost by evaporation on heating, and (c) during impregnation, the pores of the Ag-deficient glass are completely filled with the silver nitrate solution, we can estimate the final volume fraction of silver.

After firing at high temperatures, the Ag-deficient glass samples often had a surface layer of crystallized SiO₂ (α -cristobalite) caused by devitrification of the silica glass. The samples were polished to remove the devitrified surface prior to the sample characterization studies and the optical measurements. For transmission-electron-microscope (TEM) and x-ray diffraction studies, the samples were polished with SiC paper (up to No. 600). Additional polishing for optical measurements was done in sequence using slurries containing 3-, 1-, and 0.5- μ m alumina powder.

B. Sample characterization

The gross silver distribution in Ag-deficient glass was studied by x-ray mapping of the elements with a JEOL JAX-35 scanning electron microscope (SEM) with an EDAX (energy dispersive analysis of x rays) attachment. The samples contained 3.6 vol % Ag after firing at 450°C for 3 h. The SEM-EDAX of a fracture surface is shown in Fig. 1. This indicates that large clumps of



FIG. 1. A "SEM-EDAX Ag element mapping" on a fracture surface of AgNO₃-impregnated Ag-deficient glass fired at 450°C for 3 h. This map shows no large clumps of silver particles.

silver are absent and that the silver appears to be distributed rather uniformly.

The entire group of impregnated Ag-deficient glass samples was examined by x-ray diffraction. A Phillips diffractometer, equipped with an AMR (Advanced Metals Research) focusing monochromator and a copper x-ray tube, was used for all diffraction work. The x-ray patterns for the interior of the samples fired at 1050 °C contain the peaks for Ag (fcc structure) superposed on an amorphous background. The intensities of these peaks are very close to those of bulk silver, and in fact the lattice constant of the Ag in our samples is found to be 4.09 Å, in agreement with that of pure silver.¹⁵ This x-ray diffraction study also shows that *no AgNO₃ is retained in any of the fired samples.*

Selected-area electron diffraction patterns, taken for some of the samples, are shown in Fig. 2. The selected area diffraction (SAD) analysis was carried out with a JEOL CX-200 scanning transmission electron microscope (STEM), where the probe diameter (determined by the electron optics) was < 50 Å. Thus, it is possible to obtain diffraction information from areas of the order of 100 Å in diameter, significantly smaller than the 3000-Å probe diameter obtainable in conventional low-voltage electron microscopes. The method also identifies the existence of Ag, and the measured lattice constant of Ag turns out to be 4.12 Å, in agreement with the x-ray diffraction study.

When using the STEM mode, the specimens were also analyzed with the EDAX attachment to determine the chemical composition. The results of the STEM-EDAX analysis for a sample fired at 800 °C ($p=0.036$) are shown in Fig. 3. The intensity axes were normalized to a common scale based on Si peaks. As shown in Fig. 3(a), the TEM-EDAX analysis on a metal particle shows that the metal particles are clearly silver. The result of a TEM-EDAX analysis on the region between silver particles is given in Fig. 3(b). While a peak corresponding to silver is shown in the figure, the signal is too weak to demonstrate that silver atoms exist in the glass matrix. The copper signal present comes from the sample holder

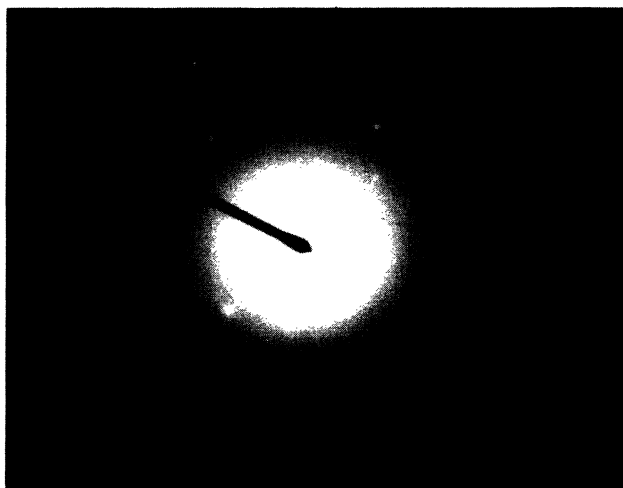


FIG. 2. A "Selected-area electron diffraction pattern" of Ag-glass composites fired at 700 °C for 20 h.

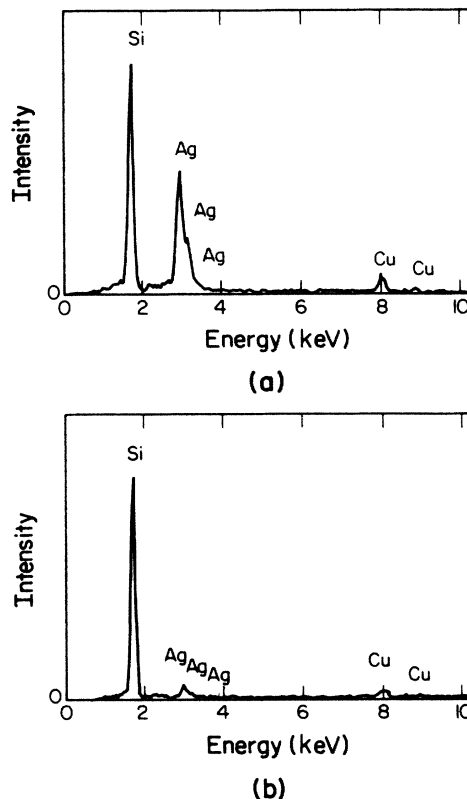


FIG. 3. A TEM-EDAX chemical analysis of the 3.6% silver glass composite fired at 800 °C. The analysis is done on (a) a large silver particle and (b) between silver particles. The TEM-EDAX analysis on a metal particle shows that the metal particle is composed of silver. The TEM-EDAX analysis between silver particles show a strong peak corresponding to a silicon component. The copper signal might come from the TEM grid.

and is probably excited by stray x-ray radiation.

The development of metal particles inside the glass was studied carefully with the scanning transmission electron microscope. Transmission-electron-microscope (TEM) specimens for particle-size analysis were taken from the interior part of the samples. A 3-mm-diameter disk was cut from the samples with a Gatan ultrasonic disk cutter and polished to a thickness of 70 μm using a disk grinder before ion milling. The angle of incidence of the incoming argon-ion beam was maintained at 15° during the first 8 h of milling and then changed to 10° until perforation of the samples occurred. After ion milling, they were coated on both sides with a carbon film several hundred angstroms thick to prevent charging effects due to the electron beam. The coated specimens were then examined in the TEM operated at 200 kV and with a beam current of about 120 μA.

Most TEM micrographs show that the silver particles are nearly spherical and that they are randomly distributed. As can be seen from Fig. 4, these particles are discrete and show no clumping or agglomeration. Stereo micrograph studies show that these particles are truly dispersed in three dimensions. The TEM micrographs also show the importance of the firing temperature in determining the microstructure of the matrix. For the

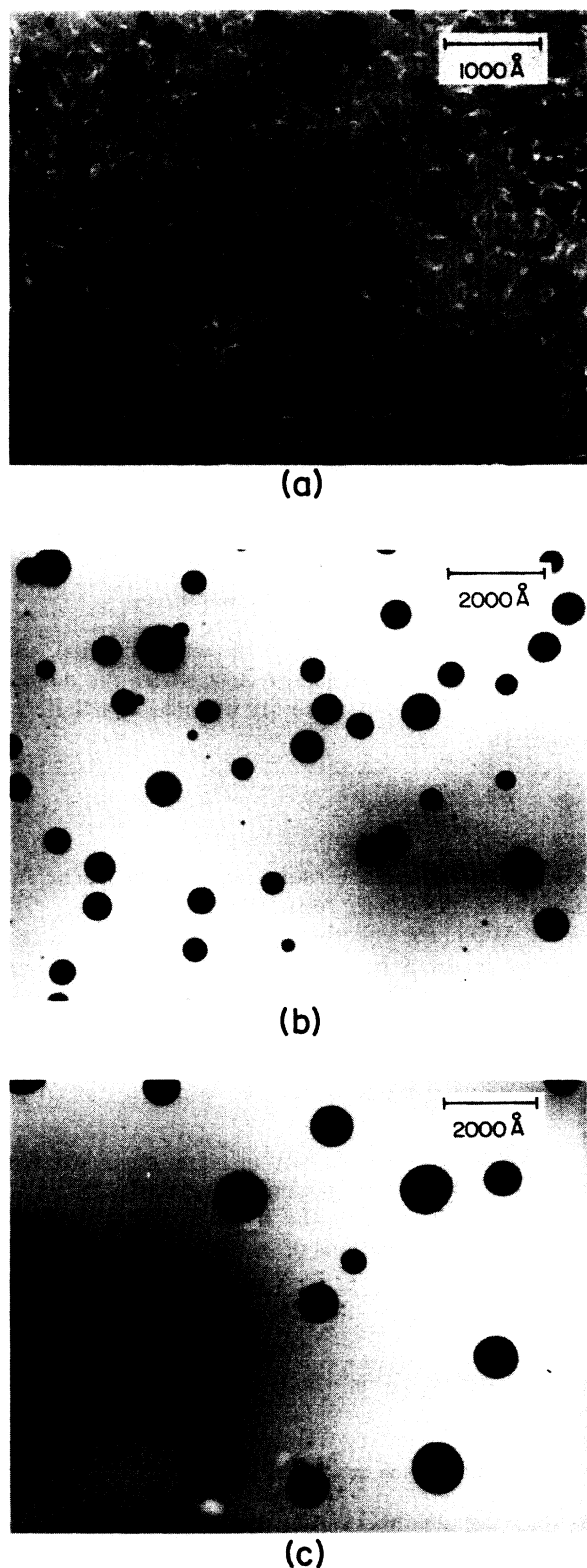


FIG. 4. TEM micrographs of a Ag-glass composite fired at the different temperatures. These specimens were fired at (a) 700°C, (b) 900°C, and (c) 1050°C for 5 h. The pore network of the Ag-deficient glass still remains at the low firing temperature, i.e., 700°C. However, the pores have completely disappeared at 900°C. The satellitelike structure of small particles shown in (c) might be explained by the Marder's correlated particle model.

samples fired below 800°C, open pore networks always exist [Fig. 4(a)]. However, the samples fired above 900°C do not show the pore network. This fact indicates that the matrix is densified before 900°C and the connected micropore network ceases to exist. This change in the microstructure of the matrix may well change the mechanism of silver transport.

To determine the size distribution of Ag particles, TEM photomicrographs were taken for at least five different spots for each sample. The photomicrographs were enlarged for data acquisition with a Carl Zeiss Videoplan image analyzer. A summary of mean radii of the silver particles in the Ag-glass composites when $p=0.036$ is given in Table I. As shown in Table I, the firing temperature is more important in determining the particle size than the firing time. For fixed firing time, the particle size becomes larger as the firing temperature increase. For Ag-glass composites fired for 5 h at 700°C, the distribution is skewed to smaller sizes, but for the samples fired at 1050°C the distribution is skewed toward larger sized particles. Near a firing temperature of 900°C, the size distribution tends to be bimodal. This bimodal distribution is due to the development of satellitelike groups of extremely small particles surrounding large particles (refer to Fig. 4). The existence of these satellitelike structures might be explained qualitatively by Marder's correlated particle-growth model,¹⁶ but no quantitative comparison is possible now. The identity of the small particles is not easy to establish with certainty because of their size, but we think that they are silver particles that are shrinking near a large silver particle as suggested by Marder's model. The number of small satellite particles reaches a maximum at 900°C, but the satellite structure still persists for a Ag-glass composite fired at 1050°C for 1200 min.

C. Optical measurements

Our Ag-glass composites have interesting color changes that depend on the heat treatment. The silver-nitrate impregnated glasses are dark brown in color after firing at 450°C, but change to a dark green color after firing at 900°C. The color of samples fired at 1050°C is a greenish gray. This change of color provided some of the motivation for the optical measurements we made on the samples.

In the past the optical properties of most Ag-glass composites have been studied by measuring the transmission spectrum. This was possible either because the metal volume fraction of these composites was very low (i.e., $p < 10^{-4}$),²⁻⁴ or the samples were very thin ($d < 10 \mu\text{m}$) with a higher metal fill fraction.⁸ However, our Ag-glass composites satisfy neither of these requirements so we could not obtain transmission spectra; our samples had $p=0.036$ and they were about 2 mm thick so they absorbed most of the incident light. Therefore, we performed reflectance measurements on our samples.

The reflectance spectra of a series of Ag-poor glass samples were recorded from 10 000 to 40 000 cm^{-1} . Ag-deficient glass containing 3.6 vol % Ag, prepared as usual, was fired for 5 h at temperatures of 450, 600, 700, 800, 900, 1000, and 1050°C. The reflectance spectra be-

TABLE I. Summary of size data for silver particles in Ag-deficient glasses having 3.6 vol % Ag. The values are given in the following order: mean plus or minus standard deviation.

| Time (min) | T (°C) | Diameter (Å) | | |
|------------|--------|--------------|---------|----------|
| | | 700 | 900 | 1050 |
| 10 | | 140±40 | 440±170 | 640±220 |
| 50 | | 140±50 | 460±160 | 630±180 |
| 300 | | 220±100 | 540±170 | 900±270 |
| 1200 | | 250±150 | 710±220 | 1160±350 |

tween 10 000 and 40 000 cm^{-1} were measured at room temperature with a BOMEM DA3.02 Fourier Transform Spectrophotometer. We used a relatively low resolution (i.e., 32 cm^{-1}) because we were primarily interested in a very broad absorption band, called the "Maxwell-Garnett resonance." Some of our measured reflection spectra are plotted in Fig. 5.

III. THEORIES

A random mixture of particles with different properties has a dielectric function which depends on position, i.e., $\epsilon = \epsilon(\mathbf{r}, \omega)$. Although the composite is completely characterized by $\epsilon(\mathbf{r}, \omega)$, this characterization is not particularly useful because the quantity of interest is the *average* response of the system to applied fields rather than the local response. However, when the length scale over which the measurement is made (in this case the wavelength of the electromagnetic radiation) is much larger than the distance over which $\epsilon(\mathbf{r}, \omega)$ fluctuates (the typical dimension of the constituent materials), the medium should behave as a homogeneous medium with an effective dielectric constant, ϵ_{eff} . Therefore if ϵ_{eff} is known for a given composite, the optical properties of that composite can be predicted. In this paper we will use two well-known effective-medium theories to calculate ϵ_{eff} , i.e., the Maxwell-Garnett theory¹ (MGT) and an effective-medium theory developed by Persson and Liebsch (PLT).⁹

Starting from a theoretical calculation of ϵ_{eff} for a composite, the complex index of refraction, $\tilde{n} = n + i\kappa$, can be obtained by using the relationship $n = (\epsilon_{\text{eff}})^{1/2}$.

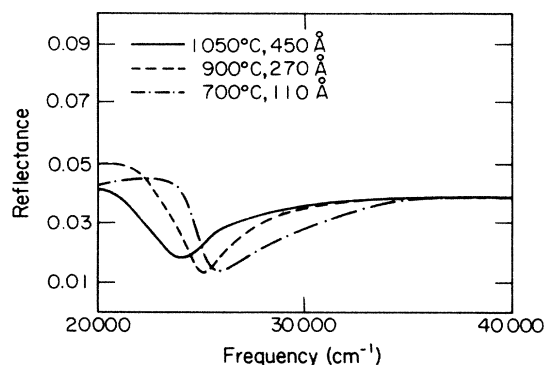


FIG. 5. The measured reflection spectra of Ag-glass composites ($p=0.036$) fired at various temperatures. The number following the temperature is the average radius of the silver particles.

Moreover, since the thickness of our sample is much larger than $1/\kappa$, the reflectance is simply related to the real and imaginary parts of the index of refraction by

$$R = \left| \frac{(n-1)^2 + \kappa^2}{(n+1)^2 + \kappa^2} \right|. \quad (1)$$

A. The Maxwell-Garnett theory

Consider the polarizability of an individual metal sphere immersed in a dielectric host where the dielectric function is ϵ_i . The polarizability of such a particle is obtained from

$$\alpha_0 = R^3 \frac{\epsilon_m - \epsilon_i}{\epsilon_m + 2\epsilon_i}, \quad (2)$$

where R and ϵ_m are the radius and the dielectric function of the metal sphere, respectively.

In the MGT, the effective dielectric function ϵ_{eff} of the composite medium is related to the polarizability of a single-metal particle via the Clausius-Mossotti equation,¹⁷ i.e.,

$$\frac{\epsilon_{\text{eff}} - \epsilon_i}{\epsilon_{\text{eff}} + 2\epsilon_i} = \frac{4}{3} \pi N \alpha_0, \quad (3)$$

where N is the number density of metal particles. From Eqs. (2) and (3), we can obtain the relationship between the dielectric function of the metal-insulator composite and the dielectric functions of its constituents:

$$\frac{\epsilon_{\text{eff}} - \epsilon_i}{\epsilon_{\text{eff}} + 2\epsilon_i} = f \frac{\epsilon_m - \epsilon_i}{\epsilon_m + 2\epsilon_i}, \quad (4)$$

where $f = 4\pi NR^3/3$ is the volume fraction of metal spheres.

B. Persson and Liebsch theory (PLT)

In deriving the MGT, the contribution to the local electric field arising from polarized particles in the vicinity of a given particle is neglected. However, the effect of the local electric field may not be negligible in real composites. Rather than deal directly with the topological disorder, Persson and Liebsch proposed a lattice-gas model in which structural disorder is replaced by substitutional disorder.⁹

Persson and Liebsch modeled a real, random, composite as a partially occupied cubic lattice of spheres and in-

cluded the dipole contributions of the spheres in the local field. By applying an alloy version of the coherent-potential approximation, the dielectric properties of such a lattice can be derived from

$$\frac{\epsilon_{\text{eff}} - \epsilon_i}{\epsilon_{\text{eff}} + 2\epsilon_i} = \frac{4}{3}\pi Nc^{-1}\alpha_{\text{eff}}, \quad (5)$$

where c is the concentration of particles in the cubic lattice of lattice constant a . Thus $c = Na^3/m$ (with m being the number of the particles in a Bravais cell). The effective polarizability of the lattice, α_{eff} , is determined self-consistently so that

$$\alpha_{\text{eff}} = c\alpha_0 \left[1 + (\alpha_0 - \alpha_{\text{eff}}) \sum_{\mathbf{q}} \frac{U(\mathbf{q})}{1 + \alpha_{\text{eff}}U(\mathbf{q})} \right]^{-1}, \quad (6)$$

where the sum over \mathbf{q} extends over the Brillouin zone of volume $m(2\pi/a)^3$ and $U(\mathbf{q})$ denotes the Fourier transform of the dipole tensor:

$$U_{\nu\mu}(\mathbf{q}) = \sum_{\mathbf{R} (\neq 0)} e^{i\mathbf{q}\cdot\mathbf{R}} (R^2\delta_{\nu\mu} - 3R_\nu R_\mu) R^{-5}. \quad (7)$$

The MGT expression is recovered from the above result if $\alpha_{\text{eff}} = c\alpha_0$, i.e., if $U(\mathbf{q})$ in Eq. (6) is set equal to zero. This approximation is equivalent to neglecting that contribution to the local electric field that arises from polarized particles in the vicinity of a given particle.

It is obvious that the specific value calculated for ϵ_{eff} of a composite medium will depend on the structure of the cubic lattice used in the calculation. However, it has been shown that the particular symmetry of the cubic lattice has very little influence on the optical properties of the composite medium due to the long-range nature of the dipole-dipole interaction.⁹ In our calculation, we chose the fcc lattice ($m=4$) and took $a=2^{3/2}R$ since the particles may touch but may not overlap.

IV. RESULTS AND DISCUSSION

To obtain specific theoretical predictions, we must choose values for ϵ_i and ϵ_m to substitute into the effective-medium expressions. For the glass matrix, we used the dispersion relation of fused quartz from the literature.¹⁸ (Over most of the frequency range we used, $\epsilon_i \approx 2.2$.) For the metal particles, we used two approaches for ϵ_m : (i) the simple Drude formula and (ii) the measured values of ϵ_m .¹⁹ In both cases the scattering rate was modified to include surface-scattering effects.

If the frequency is below that for an interband transition, metals are expected to display free-electron behavior and to satisfy the simple Drude model. The reflection spectrum, predicted by the MGT using the simple Drude formula [MGT(ϵ_{Drude})], for a Ag-glass composite with small Ag particles (with mean diameter of 110 Å) is given in Fig. 6. The calculated reflectance shows an intense peak corresponding to the Maxwell-Garnett resonance, which is usually located at $\omega_p/(2\epsilon_i + 1)^{1/2}$ (i.e., about 31 000 cm^{-1} where $\omega_p = 72\,000 \text{ cm}^{-1}$ and $\epsilon_i \approx 2.2$). [The Maxwell-Garnett

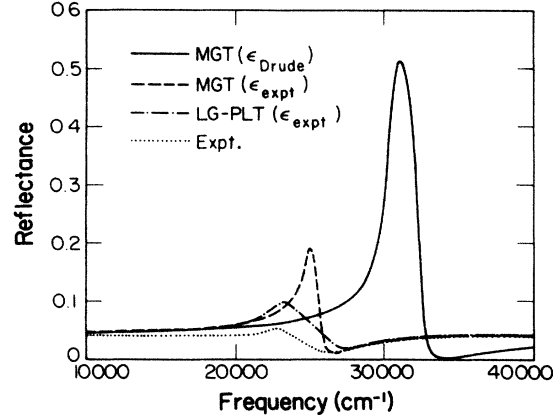


FIG. 6. The measured and calculated reflection spectra of a Ag-glass composite ($p=0.036$) fired at 700°C for 5 h.

resonance occurs because the polarization becomes very large at a certain frequency. In other words, the peak position of the Maxwell-Garnett resonance can be derived from Eq. (2) by setting $\epsilon_m + 2\epsilon_i$ equal to 0.] However, the peak position calculated in this manner is located at 31 000 cm^{-1} , higher than that observed. Moreover, the reflectance associated with this calculated resonance peak is much larger than our measured value.

The sizeable disagreement between the experimental peak position and that calculated with the MGT(ϵ_{Drude}) comes mainly from neglecting the contribution of interband transitions to ϵ_m . Due to an interband transition, the real part of ϵ_m will increase by $\delta\epsilon'_m$, shifting the peak position toward lower frequencies, i.e., from about $\omega_p/(2\epsilon_i + 1)^{1/2}$ to $\omega_p/(2\epsilon_i + 1 + \delta\epsilon'_m)^{1/2}$.

To include this interband transition, we used the measured values of ϵ_m by Johnson and Christy,²⁰ modified to account for size-dependent electron scattering in the Drude contribution to the dielectric function by writing

$$\epsilon_m(\omega) = \epsilon_{\text{expt}}(\omega) - \epsilon_b^D(\omega) + \epsilon_p^D(\omega). \quad (8)$$

Here ϵ_{expt} denotes the experimentally determined dielectric constant and the two Drude terms are given by Eq. (8) and

$$\epsilon_b^D(\omega) = 1 - \omega_p^2 / \omega(\omega + i/\tau_b). \quad (9)$$

The calculated reflection spectrum of a Ag-glass composite, using the MGT with the measured ϵ_m in Eq. (8) [MGT(ϵ_{expt})], is also given in Fig. 6. The inclusion of the interband transition reduces the peak in the reflection spectrum and shifts its position to lower frequency. It is obvious that the MGT(ϵ_{expt}) describes our experimental results much better than the MGT(ϵ_{Drude}); however, there is still a lot of room for improvement.

The inclusion of the interband transition also produces a red shift of the peak of the absorption spectrum displayed in Fig. 7. Comparison of Fig. 6 with Fig. 8(a) shows that the minimum (dip) of the reflection spectrum occurs near the frequency where $n=1$. [From Eq. (1), it

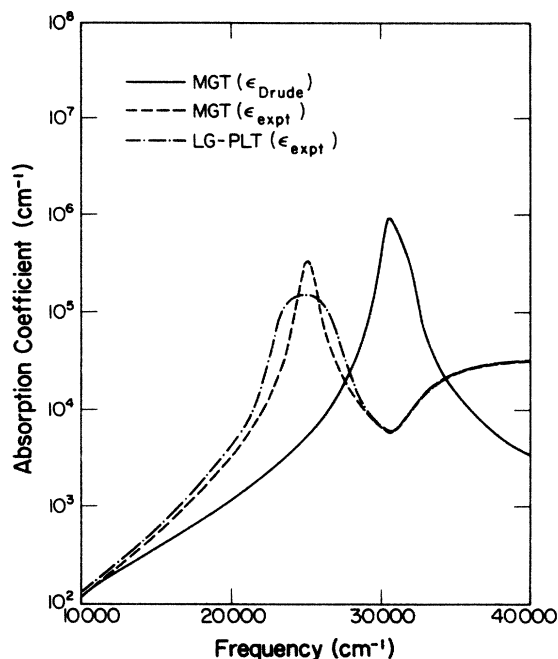


FIG. 7. The calculated absorption spectra of a Ag-glass composite (fired at 700°C for 5 h) using various models.

is clear that the dip in R will occur around $n=1$ if $\kappa \ll 1$.]

Both the MGT and the PLT use the Clausius-Mossotti equation as their starting point. However, for the MGT, the contribution to the local electric field arising from the polarized particles in the vicinity of a given particle is neglected [i.e., $U(\mathbf{q})=0$ in Eq. (6)]. Actually, for a cubic array of particles,²¹ these fields do indeed cancel so that the application of the Clausius-Mossotti equation in its simplest form is justified. However, in many real composite materials, the metal particles are randomly located inside the insulator, and this local-field cancellation is not perfect. To include the local-field effects, we used Persson and Liebsch's lattice-gas model [PLT(ϵ_{expt})] to calculate ϵ_{eff} . The value of ϵ_m used in our calculation of ϵ_{eff} was taken from Eq. (8) in order to include interband transitions. The calculated reflectance spectrum for a sample with mean Ag particle diameter of 110 Å (a sample fired at 700°C for 5 h) is given in Fig. 6.

Due to the long-range nature of the dipole coupling in the local field, the PLT predicts broader resonance than the MGT. The broadening is highly asymmetric and

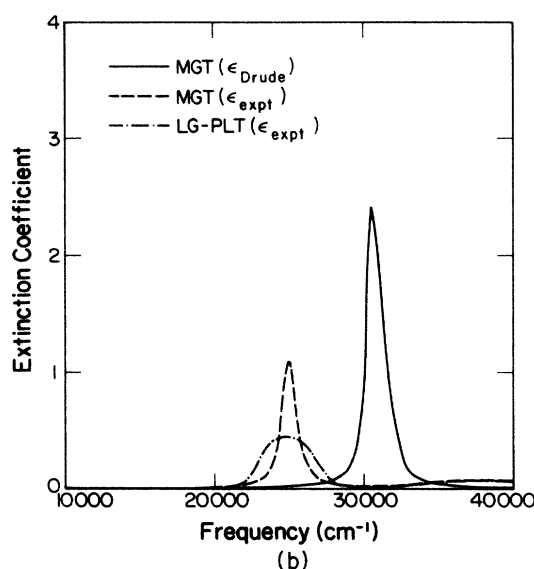
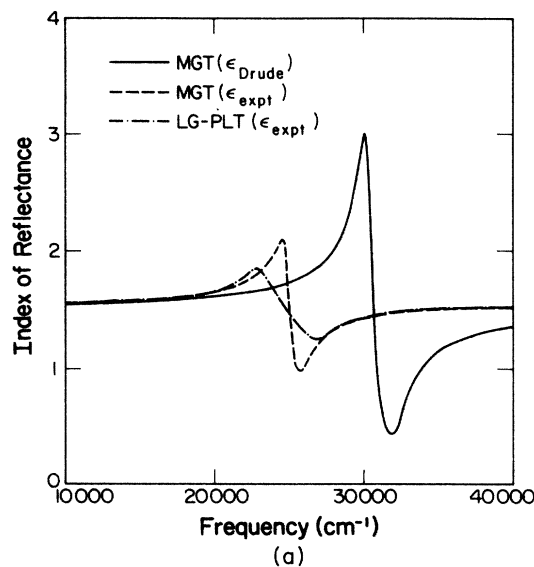


FIG. 8. (a) The calculated reflectance for a Ag-glass composite (fired at 700°C for 5 h). (b) The calculated extinction coefficients for the Ag-glass composite.

produces an effective red shift of the absorption spectrum (Fig. 6). Thus the effective red shift of a peak in either the absorption or reflectance spectrum, and the associated broadening of the peaks, are both due to the

TABLE II. Summary of the dip positions in the reflection spectra.

| T (°C) | Mean radius (Å) | Experimental ω_{min} (cm^{-1}) | MGT(ϵ_{expt}) ω_{min} (cm^{-1}) | PLT(ϵ_{expt}) ω_{min} (cm^{-1}) |
|-------------|--------------------|--|---|---|
| 450 | 25 | 29 000±100 | 27 100±10 | 27 570±10 |
| 600 | 70 | 26 700±100 | 26 560±10 | 27 280±10 |
| 700 | 110 | 26 000±100 | 26 470±10 | 27 230±10 |
| 800 | 185 | 25 200±100 | 26 400±10 | 27 200±10 |
| 900 | 270 | 25 200±100 | 26 380±10 | 27 180±10 |
| 1000 | 380 | 25 000±100 | 26 360±10 | 27 180±10 |
| 1050 | 450 | 24 300±100 | 26 360±10 | 27 180±10 |

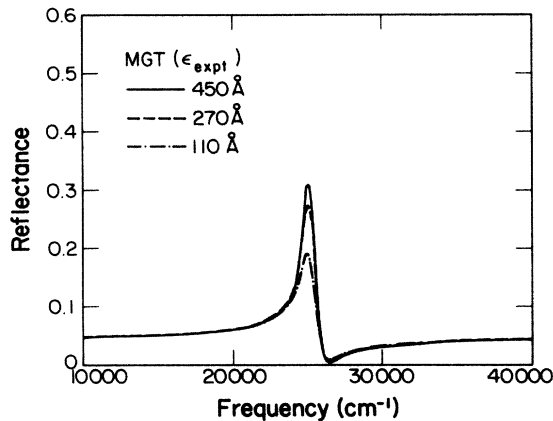


FIG. 9. The calculated reflection spectra, using the MGT(ϵ_{expt}), for Ag-glass composites fired at various temperature.

nonzero local field of the randomly distributed metal particles.

Compared to the MGT(ϵ_{expt}), the PLT (ϵ_{expt}) predicts a peak position of the reflection spectrum that is much closer to the measured peak. Moreover, the height of the peak (when compared to the MGT) is reduced, also in agreement with the experimental data. From Fig. 6, it is clear that the PLT(ϵ_{expt}) gives a much better description of the measured reflection spectrum than does the MGT(ϵ_{expt}). This fact indicates that the local-field effects of the metal particles are quite important for our composites. The strong discrepancy of the experimental absorption and that of the MGT(ϵ_{expt}), observed by Sarkar *et al.*,⁶ might be explained by these local-field effects. However, the observation of red shift does not agree with the experiments on the Au-SiO₂ composites prepared by the "tandem-sputtering" technique.¹²

The size effects associated with experiments on small metal particles have been an interesting issue for over a century,²² and it is worthwhile to examine the effects of particle size on both our experimental data and theoretical analysis. The TEM studies showed that the silver particles became larger as we fired the Ag-glass composites at higher temperatures. As can be seen in Fig. 5, the position of the dip in the reflectance depends strongly on the size of Ag particles and provides the virtual color difference between the samples. As the firing temperature is increased, the position of dip shifts to lower frequency significantly. However, as shown in Figs. 9 and 10, neither the MGT(ϵ_{expt}) nor the PLT(ϵ_{expt}) predict such evident changes in the dip position. As shown in Table II, both theories do predict a shift of dip position to lower frequency as the particle size increases, but the size of the calculated shift is much too small to explain our experimental data. The experimental effect is large enough that it could be used to quantitatively predict particle size.

Of the two theories used here, the PLT(ϵ_{expt}) provides a description of the reflection spectrum that is superior to the MGT(ϵ_{expt}) description, as shown in Fig. 6. Nevertheless, PLT(ϵ_{expt}) cannot explain our measured reflection spectrum quantitatively. In particular, it appears that the influence of particle size on the dip posi-

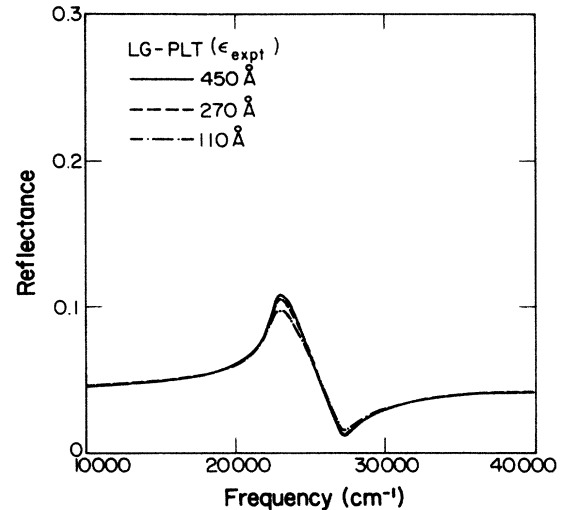


FIG. 10. The calculated reflection spectra, using the PLT(ϵ_{expt}), for Ag-glass composites fired at various temperature.

tion of the reflection spectrum cannot be satisfactorily explained by the PLT(ϵ_{expt}). This discrepancy might, however, be due to silver particles in our composite not being distributed randomly. The satellitelike structures observed in our TEM studies indicate that the positions of some of silver particles *are* correlated. Therefore, as a further study, it would be interesting to investigate the connection between the observed change of dip position in the reflection spectrum and correlations between the positions of the metal particles.

In summary, we prepared Ag-glass composites by impregnating porous glass with a AgNO₃ solution (followed by reduction and densification at various temperatures). The characteristics of these Ag-glass composites were studied by an x-ray diffractometer and electron microscopy, while the development of the metal particles inside the glass were studied carefully by a transmission electron microscope. The reflectance spectra of our Ag-glass composites were measured at low resolution between 10 000 and 40 000 cm⁻¹ at room temperature. To understand the measured reflectance, we used two different theoretical approaches; the Maxwell-Garnett theory (MGT) and a lattice-gas model developed by Persson and Liebsch (PLT). The PLT did predict the red shift, broadening, and reduction of the peak in the reflectance much better than the MGT. However, the PLT cannot explain the size-dependent characteristics of our measured spectrum, especially changes of the dip position due to particle size.

ACKNOWLEDGMENTS

We would like to thank Yi Song for his help with the optical measurements. We are pleased to acknowledge Hendrik O. Colijn for his help with the transmission electron microscopy. The financial support of the National Science Foundation through a grant to the Ohio State University Materials Research Laboratory (DMR-83-16989) and Grant No. DMR-84-05403 is gratefully acknowledged.

- ¹J. C. Maxwell-Garnett, *Philos. Trans. R. Soc. London* **203**, 385 (1904); **205**, 237 (1906).
- ²R. D. Maurer, *J. Appl. Phys.* **29**, 29 (1958); R. H. Doremus, *J. Chem. Phys.* **40**, 2389 (1964); **42**, 414 (1965); R. H. Doremus and A. M. Turkalo, *J. Mater. Sci.* **11**, 903 (1976).
- ³D. Chakravorty, *J. Non-Cryst. Solids* **15**, 191 (1974); G. C. Das, T. K. Reddy, and D. Chakravorty, *J. Mater. Sci.* **13**, 2211 (1978).
- ⁴The optical properties of "metal colloids" in ionic crystals were reviewed by A. E. Hughes and S. C. Jain, *Adv. Phys.* **28**, 717 (1979).
- ⁵A. J. Sievers, in *Solar Energy Conversion*, edited by B. O. Seraphin (Springer, Berlin, 1979), p. 5.
- ⁶P. Sarkar, J. Kumar, and D. Chakravorty, *J. Mater. Sci.* **18**, 250 (1983).
- ⁷A number of references may be found in T. W. Noh, Y. Song, S. I. Lee, J. R. Gaines, H. D. Park, and E. R. Kreidler, *Phys. Rev. B* **33**, 3793 (1986).
- ⁸U. J. Gibson, H. G. Craighead, and R. A. Buhrman, *Phys. Rev. B* **25**, 1449 (1982).
- ⁹B. N. J. Persson and A. Liebsch, *Solid State Commun.* **44**, 1637 (1982); A. Liebsch and B. N. J. Persson, *J. Phys. C* **16**, 5375 (1983); A. Liebsch and P. V. Gonzalez, *Phys. Rev. B* **29**, 6907 (1984).
- ¹⁰W. Lamb, D. M. Wood, and N. W. Ashcroft, *Phys. Rev. B* **21**, 2248 (1980); Y. Kantor and D. J. Bergman, *J. Phys. C* **15**, 2033 (1982); J. M. Gerardy and M. Ausloos, *Phys. Rev. B* **26**, 4703 (1982).
- ¹¹R. H. Doremus, *J. Chem. Phys.* **42**, 414 (1965); R. W. Cohen, G. D. Cody, M. D. Coutts, and B. Abeles, *Phys. Rev. B* **8**, 3689 (1973); L. Genzel and T. P. Martin, *Surf. Sci.* **34**, 33 (1973); T. Welker and T. P. Martin, *J. Chem. Phys.* **70**, 5683 (1979); U. Kreibig, A. Althoff, and H. Pressmann, *Surf. Sci.* **106**, 308 (1981); C. G. Granqvist, *J. Phys.* **42**, 247 (1981).
- ¹²W. J. Kaiser, E. M. Logothetis, and L. E. Wenger, *J. Phys. C* **18**, L837 (1985).
- ¹³S. I. Lee, T. W. Noh, K. Cummings, and J. R. Gaines, *Phys. Rev. Lett.* **55**, 1626 (1985).
- ¹⁴H. Tanaka, *J. Non-Cryst. Solids* **65**, 301 (1984).
- ¹⁵*American Institute of Physics Handbook*, edited by Dwight E. Gray (McGraw-Hill, New York, 1982), Sec. 9.
- ¹⁶M. Marder, *Phys. Rev. Lett.* **55**, 2953 (1985).
- ¹⁷J. D. Jackson, *Classical Electrodynamics* (Wiley, New York, 1962), Chap. 4.
- ¹⁸*Optical Materials Properties, Handbook of Electronic Materials*, edited by A. J. Moses (Plenum, New York, 1971), p. 68.
- ¹⁹G. R. Parking, W. E. Lawrence, and R. W. Christy, *Phys. Rev. B* **23**, 6408 (1981).
- ²⁰P. B. Johnson and R. W. Christy, *Phys. Rev. B* **6**, 4370 (1972).
- ²¹See, for example, N. W. Ashcroft and N. D. Mermin, *Solid State Physics* (Holt, Rinehart and Winston, New York, 1976), p. 542.
- ²²A number of references may be found in U. Kreibig, *Z. Phys.* **B 31**, 39 (1978).

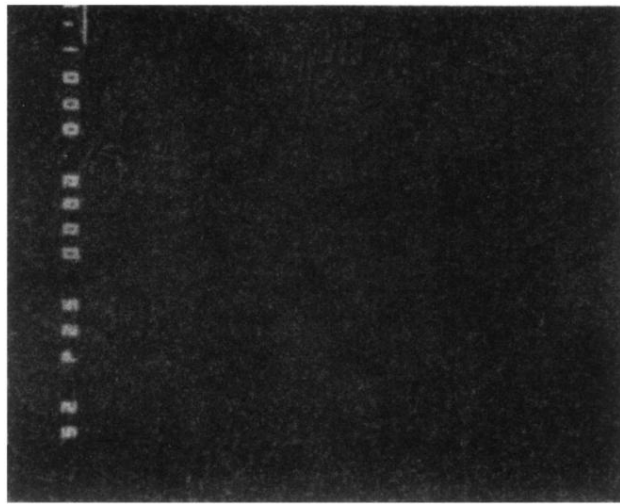


FIG. 1. A "SEM-EDAX Ag element mapping" on a fracture surface of AgNO_3 -impregnated Ag-deficient glass fired at 450°C for 3 h. This map shows no large clumps of silver particles.

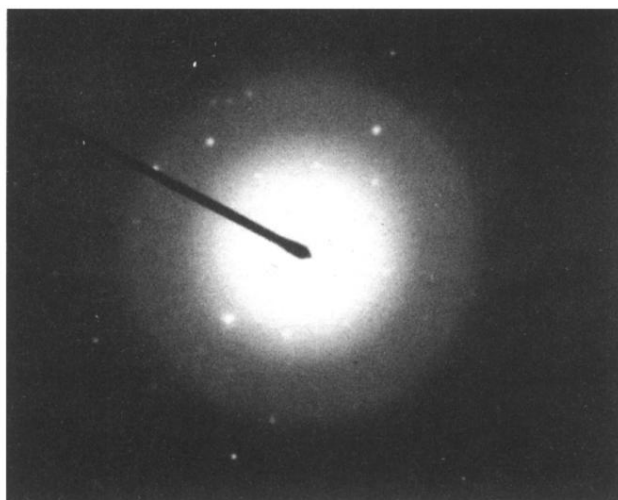
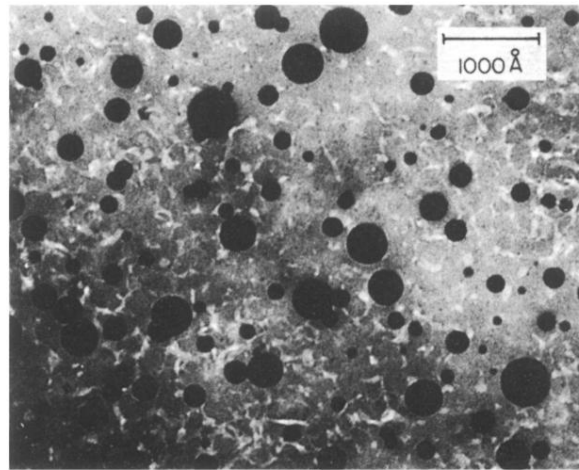
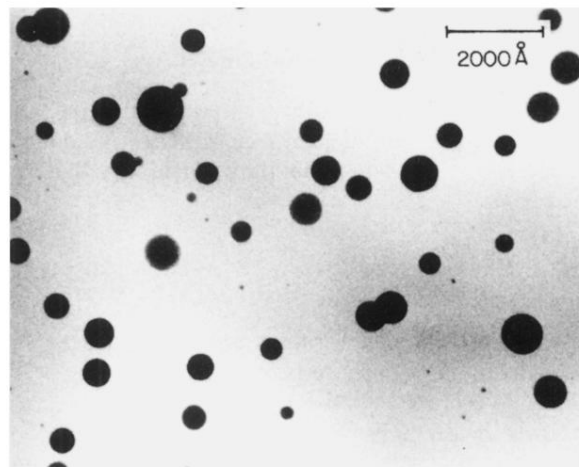


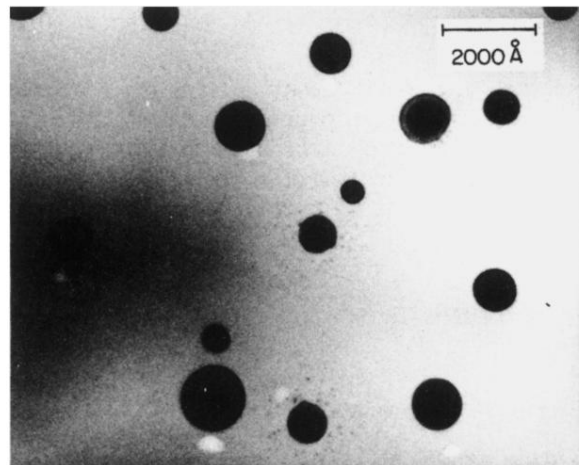
FIG. 2. A "Selected-area electron diffraction pattern" of Ag-glass composites fired at 700°C for 20 h.



(a)



(b)



(c)

FIG. 4. TEM micrographs of a Ag-glass composite fired at the different temperatures. These specimens were fired at (a) 700°C, (b) 900°C, and (c) 1050°C for 5 h. The pore network of the Ag-deficient glass still remains at the low firing temperature, i.e., 700°C. However, the pores have completely disappeared at 900°C. The satellitelike structure of small particles shown in (c) might be explained by the Marder's correlated particle model.